An exploration of pathways involved in lung carcinoid progression using gene expression profiling

Carcinogenesis vol.00 no.00 p.1 of 12, 2013
doi:10.1093/carcin/bgt271
Advance Access publication August 8, 2013

An exploration of pathways involved in lung carcinoid progression using gene expression profiling

Dorian R.A.Swarts*,†, Leander Van Neste[1,†], Mieke E.R.Henfling, Ivo Eijkenboom, Paul P.Eijk[2], Marie-Louise van Velthuysen[3], Aryan Vink[4], Marco Volante[5], Bauke Ylstra[2], Wim Van Criekinge[6], Manon van Engeland[7], Frans C.S.Ramaekers and Ernst-Jan M.Speel[7]

Department of Molecular Cell Biology, GROW – School for Oncology & Developmental Biology, Maastricht University Medical Center, PO Box 616, 6200 MD Maastricht, The Netherlands, [1]MDxHealth, Irvine, CA, USA, [2]Department of Pathology, VU University Medical Center, Amsterdam, The Netherlands, [3]Division of Pathology, Netherlands Cancer Institute, Amsterdam, The Netherlands, [4]Department of Pathology, University Medical Center, Utrecht, The Netherlands, [5]Division of Pathology, Department of Oncology, University of Turin at San Luigi Hospital, Orbassano, Turin, Italy, [6]Laboratory of Bioinformatics and Computational Genomics, Ghent University, Ghent, Belgium and [7]Department of Pathology, GROW – School for Oncology & Developmental Biology, Maastricht University Medical Center, PO Box 616, 6200 MD Maastricht, The Netherlands

*To whom correspondence should be addressed. Tel: +31 43 3882998; Fax: +31 43 3884151;
Email: d.swarts@maastrichtuniversity.nl

Pulmonary carcinoids comprise a well-differentiated subset of neuroendocrine tumors usually associated with a favorable prognosis, but mechanisms underlying disease progression are poorly understood. In an explorative approach to identify pathways associated with progression, we compared gene expression profiles of tumors from five patients with a favorable and five with a poor disease outcome. Differentially expressed genes were validated using quantitative real-time PCR on 65 carcinoid tumors, in combination with survival analysis. One of the identified pathways was further examined using immunohistochemistry. As compared with other chromosomal locations, a significantly higher number of genes downregulated in carcinoids with a poor prognosis were located at chromosome 11q ($P = 0.00017$), a region known to be frequently lost in carcinoids. In addition, a number of upregulated genes were found involved in the mitotic spindle checkpoint, the chromosomal passenger complex (CPC), mitotic kinase CDC2 activity and the BRCA-Fanconi anemia pathway. At the individual gene level, *BIRC5* (survivin), *BUB1*, *CD44*, *IL20RA*, *KLK12* and *OTP* were independent predictors of patient outcome. For survivin, the number of positive nuclei was also related to poor prognosis within the group of carcinoids. Aurora B kinase and survivin, major components of the CPC, were particularly upregulated in high-grade carcinomas and may therefore comprise therapeutic targets for these tumors. To our knowledge, this is the first expression profiling study focusing specifically on pulmonary carcinoids and progression. We have identified novel pathways underlying malignant progression and validated several genes as being strong prognostic indicators, some of which could serve as putative therapeutic targets.

Introduction

Pulmonary carcinoids are well-differentiated neuroendocrine tumors with little relation to cigarette smoking (1). In contrast to other lung neuroendocrine neoplasms (NENs), i.e. the poorly differentiated large cell neuroendocrine carcinoma and small cell lung cancer (SCLC), carcinoids are characterized by a low metastatic rate and a relatively favorable prognosis. According to the World Health Organization, based on histopathologic features, lung carcinoids are subclassified as typical carcinoid or atypical carcinoid (AC) (2), and the latter being characterized by a more aggressive clinical behavior and a lower 5 year survival (3). Pulmonary carcinoids are considered as separate entities and transitions from typical to atypical subtypes have not been reported (1). Metastases will usually develop in regional lymph nodes, but also at distant sites including liver, bone, brain, subcutaneous tissue and breast (1,3). Clinical management of metastatic disease remains difficult and a curative treatment strategy for these cases is not available (1,4). Metastatic lung carcinoids are usually subjected to SCLC treatment regimens, but their response rate is considerably lower (4).

Pulmonary carcinoids have been reported in the context of the multiple endocrine neoplasia type 1 syndrome and a number of sporadic tumors have a mutation of the *MEN1* gene (5,6). We have previously described a tentative model for the tumorigenesis of pulmonary carcinoids (1). However, although clinical and molecular parameters with prognostic value have been described previously (1,7–10), the processes underlying malignant progression of lung carcinoids, defined as extensive spread of the disease and/or distant metastasis, are poorly understood (1). We have previously found that deletion of chromosome 11q22.3–q25 is associated with ACs and a poor disease outcome (9). Furthermore, aggressive carcinoids may show a high Bcl-2/Bax ratio, indicating that apoptosis may be hampered (11). Ki-67 may or may not be enhanced in cases with a poor disease outcome (12,13), whereas CD44 may be lost in aggressive cases (10,14). To identify molecular parameters that distinguish tumors with a favorable outcome from those with a poor clinical outcome, genome-wide gene expression profiling has proven helpful (15). However, only few of such studies that included lung carcinoids have been published (16–20), whereas none of these studies focused specifically on carcinoid tumors and progression (1).

In the underlying study, differentially expressed genes and associated pathways involved in carcinoid progression were identified using high-resolution gene expression microarrays on carcinoids from patients with a very poor disease outcome on the one hand and those of patients with a favorable outcome on the other. These pathways, as well as the prognostic value of a number of candidate genes, were validated by quantitative real-time PCR (qRT–PCR) as well as immunohistochemistry. The findings were also related to the results from high-resolution array comparative genomic hybridization (array CGH) assays.

Materials and methods

For more information, see Supplementary Materials and methods, available at *Carcinogenesis* Online.

Tumor material and case selection

In order to discover novel genes associated with pulmonary carcinoid progression, 10 pulmonary carcinoids were subjected to microarray experiments. Frozen tissue (≥70% tumor cells) was selected from five tumors of carcinoid patients with a favorable prognosis (all ≥7 year disease-free survival without metastasis or recurrence) and five from patients with a very poor disease outcome (all distant metastasis or deceased ≤3 years after diagnosis) (Table I).

Frozen tissue material (≥70% tumor cells) from 55 additional carcinoids and 16 high-grade neuroendocrine carcinomas was collected for qRT–PCR as described previously (10). In addition, nine neuroendocrine cell lines and four normal tissues (adrenal gland, liver, lung and pancreas) were analyzed (10). Formalin-fixed paraffin-embedded material of 65 pulmonary NENs (50 carcinoids and 15 high-grade carcinomas) was included for immunohistochemistry.

Abbreviations: ABk, Aurora B kinase; AC, atypical carcinoid; CGH, comparative genomic hybridization; CIN, chromosomal instability; CPC, chromosomal passenger complex; FA, Fanconi anemia; mRNA, messenger RNA; MSC, mitotic spindle checkpoint; NEN, neuroendocrine neoplasm; NSCLC, non-small cell lung cancer; qRT–PCR, quantitative real-time PCR; SCLC, small cell lung cancer.

†These authors contributed equally to this work.

Table I. Patient and tumor characteristics (A), Ki-67 proliferative index (B) and array CGH data (C) of the 10 carcinoid cases used for microarray analyses

Case	Poor outcome					Favorable outcome				
	1	2	3	4	5	6	7	8	9	10
(A) Patient and tumor characteristics										
Subtype	AC	AC	AC	AC	AC	TC	AC	AC	TC	TC
Sex	F	M	M	F	M	F	F	F	M	F
Age at surgery	58	59	63	68	69	63	22	26	60	47
Tumor diameter (cm)	1	5.5	6.2	3	3	1.8	2.5	3	1.8	2.3
Stage at surgery	IA	IV	IV	Unknown	IV	IA	IA	IA	Unknown	Unknown
Follow-up (months)	36	144	49	35	27	141	230	135	90	118
Disease status	D	DOD	DOD	D	DOD	NED	NED	NED	NED	NED[a]
Metastases	Unknown	Mediastinum, diaphragm, sternum	Liver[b], spleen	Unknown	Skin, lung[b], spine, brain	None	None	None	None	None
Ploidy[c]	$n = 2$	$n = 2$	$n = 2$	$n = 2$	$n = 2$	$n = 2$	$n = 2$	$n = 2$	$n = 2$	$n = 2$
(B) Ki-67 (%)										
FFPE		6.4	2.3		7.2	0.2	1.4	5.1	1.2	4.2
Frozen	32.5			30.8	7.2					
(C) Array CGH results										
Number of chromosomal alterations >10 Mb	16	0	11	27	8	0	5	11	0	2[d]
Gains (>10 Mb)	5p, 6p		7pq[e]	1q, 3p, 6p, 8q, 12q, 14q, 16q, 20q	16pq, 19pq, 21q		Xpq	16pq		
Losses (>10 Mb)	3p, 5q, 9p, 10q, 11q, 12p, 13q, 17p, Xq		6pq, 11pq	2q, 6q, 11pq, 13q, 14q, 17p, 18pq, 21q, 22q	3p, 13q			1p, 2q, 6pq, 13q, 18pq, Xpq		19p, 22q
Amplifications (≥2 cases)		3q26.1	7p22.3	7p22.3, 9q32, 14q32.33		9q32, 14q32.33	14q32.33	3q26.1	3q26.1	3q26.1
Homozygous deletions (≥2 cases)	8p11.22, Xq26.3			8p11.22, 17q21.31	8p11.22		8p11.22, 17q21.31	Xq26.3		

D, deceased; DOD, died of disease; F, female; FFPE, formalin-fixed paraffin-embedded; M, male; Mb, mega base; NED, no evidence of disease; TC, typical carcinoid.

[a]This patient had an unrelated lymphoma.

[b]Material from this metastasis used instead of primary tumor.

[c]As determined by FISH using centromere probes for chromosomes 1, 3, 7 and 11.

[d]Multiple deletions combined >10 Mb, but individually not surpassing this criterion (see Figure 4).

[e]The gain of chromosome 7 in this metastatic carcinoid tumor was not present in the primary tumor, which was subjected to array CGH in a previous study (9) (case 27).

These latter cases comprise a subset of the tumors described in detail in a previous study (10). The current study meets the criteria of the code for proper secondary use of human tissue in The Netherlands (Federation of Medical Scientific Societies, The Netherlands; 2003).

Sample preparation and messenger RNA expression profiling

RNA was isolated from the tumor tissues using the RNeasy Mini Kit (Qiagen GmbH, Hilden, Germany). RNA integrity was tested by chip analysis using the Bioanalyzer 2100 (Agilent Technologies, Santa Clara, CA) and was >7 for all samples. The RNA samples were converted to complementary DNA, subsequently labeled during complementary RNA conversion and hybridized onto Agilent Human* GE 4x44K v2 Microarrays (Agilent Technologies), according to the manufacturer instructions (Two-Color Microarray-Based Gene Expression Analysis–Low Input Quick Amp Labeling protocol, version 6.5) and not including the RNA Spike-In kit step (Step 1). Hybridization of each sample was performed in duplicate, with dye swap, once using cyanine-3 and once using cyanine-5 fluorescent as a dye for the tumor samples. Universal Human Reference RNA (Stratagene, Agilent Technologies, Santa Clara, CA) from a cell line pool expressing 70–80% of all human genes, was hybridized onto each microarray slide as a control. The raw microarray data are available in the ArrayExpress database (http://www.ebi.ac.uk/arrayexpress) under accession number E-MEXP-3790.

Gene selection procedures

Data processing and analysis were performed using *R* (21). Loess normalization and minimal background subtraction were carried out to correct for imbalance between the fluorescent dyes. After initial processing, the signals of four replicates (i.e. samples 2 and 3 labeled with cyanine-5 and samples 4 and 5 labeled with cyanine-3) showed a generally deviant behavior, and were therefore excluded from further analysis. The expression profile was determined for each sample by calculating the natural logarithm of the average across all replicates. For the four samples without available replicate, the expression profile was based on a single array.

Because of the low number of samples included in the expression array analyses, a stringent selection was performed to determine differentially expressed genes between the two groups (see Supplementary Table S1, available at *Carcinogenesis* Online). Subsequently, the $\log_2$ ratio of all these differential expression ratios was calculated and differentially expressed genes in the poor prognosis group were identified using a cutoff of 0.5 on the $\log_2$ scale. This resulted in 307 unique genes (as identified from 681 probes, i.e. 1.5%, on the microarray) that were differentially expressed between the carcinoids with a poor and a favorable disease outcome (arranged according to median fold change in Supplementary Table S1, available at *Carcinogenesis* Online). A selection of 71 top candidate genes is shown in Table II.

Pathway analysis

The 307 altered genes between the two prognostic groups (Supplementary Table S1, available at *Carcinogenesis* Online) were subjected to pathway analysis using DAVID (http://david.abcc.ncifcrf.gov/; DAVID Bioinformatics Resources 6.7, NIAID, NIH, Bethesda, MD). Furthermore, the literature was thoroughly screened in search of additional relationships between top candidate genes. Interactions between candidate genes were also identified using the online BioGRID tool (http://thebiogrid.org; version 3.1).

Quantitative RT–PCR

Results of the gene expression microarrays were validated using qRT–PCR on 65 carcinoids (including the 10 cases subjected to gene expression profiling) and 16 high-grade lung NENs. RNA processing and qRT–PCR were performed as described previously (10), using the primers listed in Supplementary Table S2, available at *Carcinogenesis* Online. These were designed to detect the housekeeping genes *ACTB*, *CYPA*, *GUSB* and *HPRT*, and the differentially expressed *BIRC5*, *BUB1*, *FANCA*, *FOLR1*, *IL20RA*, *KLK12*, *MT1F* and *PCK1* genes. The qRT–PCR procedure is further described in the Supplementary Data, available at *Carcinogenesis* Online.

Immunohistochemistry

One of the identified pathways, i.e. the chromosomal passenger complex (CPC), was further examined using immunohistochemistry for Aurora B kinase (ABk) and survivin (the *BIRC5* gene product) on formalin-fixed paraffin-embedded and frozen material of 50 carcinoids and 15 high-grade neuroendocrine carcinomas. The following antibodies were used: (i) mouse anti-ABk monoclonal antibody, clone 6/AIM-1 (BD Transduction Laboratories, Lexington, KY); (ii) rabbit anti-survivin polyclonal antibody (AF886; R&D systems, Boston, MA). Mouse anti-Ki-67 monoclonal antibody, clone MIB-1 (Dako, Glostrup, Denmark) was used to determine proliferation in the 10 cases subjected to gene expression profiling. The assay conditions are described in the Supplementary Data, available at *Carcinogenesis* Online.

The immunohistochemical staining patterns were evaluated as follows. Frequencies of ABk- and survivin-positive nuclei were calculated after manually counting ≥500 nuclei. Cytoplasmic positivity was scored when diffusely present with a considerable intensity. Frequencies of Ki-67-positive cells were calculated using an automated cell-counting approach.

Array CGH

To identify chromosomal alterations in the 10 cases subjected to gene expression profiling (Table IA), DNA isolated from these cases was hybridized onto NimbleGen Human CGH 3x720K Whole-Genome Tiling v3.0 Arrays (Roche NimbleGen, Madison, WI), as described in the Supplementary Data, available at *Carcinogenesis* Online. The raw array CGH data are available in the ArrayExpress database (http://www.ebi.ac.uk/arrayexpress) under accession number E-MEXP-3806.

Correlation of molecular parameters with clinical follow-up

Possible correlations between clinical data and qRT–PCR results were determined using IBM SPSS Statistics (version 20.0.0; IBM, New York, NY). Survival curves were created using the Kaplan–Meier method. Cutoff points for gene expression levels and frequencies of nuclear immunoreactivity were determined using area under the receiver operating characteristic curve analysis. The log-rank test was used to test for differences between subgroups. Overall survival was calculated from the date of diagnosis until patient's death or until the last date the patient was known to be alive. Multivariate analyses were performed using Cox regression, including age at diagnosis, diameter, histopathology, sex and qRT–PCR results for the individual genes. Differences in gene and protein expression levels for different tumor subgroups were determined using the Student's *t*-test. The chi-square test was used to calculate the overrepresentation of downregulated genes on chromosome 11q. All *P* values were considered statistically significant if ≤0.05 for two-sided tests.

Results

In order to discover novel genes associated with pulmonary carcinoid progression, frozen material from five pulmonary carcinoids with a favorable prognosis and five with an adverse prognosis was retrieved from our archives. Clinical data and tumor characteristics of these cases are shown in Table IA. All cases were consensus classified as pulmonary carcinoids by at least two pathologists according to the World Health Organization classification (2). Our subjects (four males, six females, mean age 54 years, range 22–69) were selected based on their disease outcome, thus irrespective of histopathologic classification into ACs and typical carcinoids, which is difficult leading to a high interobserver variation (22). In accordance with the literature (9,23), the ploidy status of these cases was found to be diploid based on FISH, whereas the MIB-1 proliferative capacity of the tumors ranged between 0 and 33% (Table IB and Supplementary Figure S1, available at *Carcinogenesis* Online). Because of the high proliferative index of cases 1 and 4, we decided to further examine the cases with a poor prognosis for *TP53* mutation, an infrequent event in pulmonary carcinoids (1). Case 1 exhibited mutation Y236C in exon 7, although the *TP53*-mutated allele was present 3–4 times less frequently than the wild-type allele. Immunohistochemistry confirmed the heterogeneity of this case since only part of the tumor cells were p53 positive (data not shown).

Identification of genes differentially expressed between pulmonary carcinoids with a favorable and a poor prognosis

Using expression profiling, 307 genes (Supplementary Table S1, available at *Carcinogenesis* Online) were found to be differentially expressed to a significant degree in the five lung carcinoids with a favorable prognosis as compared with the five with a poor outcome. A selection of 71 annotated candidates with a median fold change ≥5 from these 307 is shown in Table II. The gene showing the strongest upregulation in cases with a poor prognosis was the *RET* proto-oncogene (10). Among the 23 genes upregulated with a median fold change ≥5 were also factors involved in cell cycle control mechanisms, including *ASPM*, *BIRC5* (survivin), *BUB1*, *CASC5* (blinkin), *CEP55*, *FANCA*, *HIST1H3B*, *ORC6L*, *RCC1* and *UBE2C*, the angiogenic growth factor *SMOC2* and the secreted serine protease *KLK12*. The strongest downregulation in cases with a poor prognosis was seen for the orthopedia homeobox gene *OTP* (10).

Table II. Differentially expressed genes between lung carcinoids with a poor and a favorable prognosis[a]

Gene abbreviation[b]	Median (poor prognosis)	Median (good prognosis)	Median fold change	Chromosomal location[c]	Gene name
Upregulated genes in carcinoids with a poor prognosis					
RET	1187.91	19.80	59.987	10q11.2	RET proto-oncogene
KLK12	233.55	10.01	23.325	19q13.33	Kalikrein 12
SMOC2	7075.18	432.61	16.355	6q27	SPARC-related modular calcium binding 2
HBB	8394.37	632.69	13.268	11p15.5	Beta-hemoglobin
POTEB	231.15	19.80	11.672	15q11.2	POTE ankyrin domain family, member B
BUB1	144.99	12.65	11.457	2q14	Budding uninhibited by benzimidazoles 1 homolog (yeast)
ORC6L	152.08	15.59	9.753	16q12	Origin recognition complex, subunit 6
METRNL	3167.14	341.29	9.280	17q25.3	METRNL meteorin, glial cell differentiation regulator-like
PTTG2	809.69	89.45	9.052	4p12	Pituitary tumor-transforming 2
FANCA	53.75	5.98	8.996	16q24.3	Fanconi anemia, complementation group A
KAZALD1	914.66	109.56	8.348	10q24.31	Kazal-type serine peptidase inhibitor domain 1
DTL	137.08	18.77	7.304	1q32	Denticleless homolog
ASPM	106.59	14.65	7.275	1q31	Asp (abnormal spindle) homolog, microcephaly associated (*Drosophila*)
RPP25	559.88	77.72	7.203	15q24.2	Ribonuclease P/MRP 25 kDa subunit
POTED	159.99	22.95	6.970	21q11.2	POTE ankyrin domain family, member D
CEP55	70.85	11.37	6.232	10q23.33	Centrosomal protein 55 kDa
BIRC5	700.49	112.55	6.224	17q25	Baculoviral IAP repeat containing 5
HBD	3095.95	508.95	6.083	11p15.5	Delta-hemoglobin
RCC1	130.10	21.43	6.072	1p36.1	Regulator of chromosome condensation 1
ARC	87.31	14.66	5.954	8q24.3	Activity-regulated cytoskeleton-associated prote
UBE2C	413.10	70.52	5.858	20q13.12	Ubiquitin-conjugating enzyme E2C
CASC5	77.08	14.23	5.417	15q14	Cancer susceptibility candidate 5
HIST1H3B	567.97	112.18	5.063	6p22.1	Histone cluster 1, H3b
Downregulated genes in carcinoids with a poor prognosis					
OTP	21.67	18 320.20	0.001	5q13.3	Orthopedia homeobox
PCK1	15.17	2357.44	0.006	6q25.1	Phosphoenolpyruvate carboxykinase 1
ASB4	21.82	2941.85	0.007	7q21–q22	Ankyrin repeat and SOCS box containing 4
FOLR1	46.28	5097.19	0.009	11q13–q14.1	Folate receptor 1
SLC45A3	22.94	2046.66	0.011	1q32.1	Solute carrier family 45, member 3
FOLR3	2.28	151.88	0.015	11q13	Folate receptor 3 (gamma)
SOD3	1042.44	60 621.59	0.017	4p15.3–p15.1	Superoxide dismutase 3, extracellular
DLG2	21.36	1020.66	0.021	11q14.1	Discs, large homolog 2
GALNT14	75.05	3175.05	0.024	2p23.1	UDP-*N*-acetyl-alpha-D-galactosamine:polypeptide *N*-acetylgalactosaminyltransferase 14
CDH3	15.30	613.45	0.025	7q22.3	Cadherin-related family member 3
IL20RA	12.37	463.20	0.027	6q23.3	IL20RA interleukin 20 receptor, alpha
SFTA3	10.04	319.08	0.031	14q13.3	Surfactant associated 3
B3GAT1	33.05	1028.62	0.032	11q25	Beta-1,3-glucuronyltransferase 1 (glucuronosyltransferase P; CD57)
KIRREL3	19.74	597.56	0.033	11q24	Kin of IRRE like 3
CD44	9.83	288.91	0.034	11p13	CD44 molecule (Indian blood group)
KLHDC8A	34.82	1019.71	0.034	1q32.1	Kelch domain containing 8A
LECT1	15.95	414.96	0.038	13q14.3	Leukocyte cell-derived chemotaxin
ADAMTS18	11.87	271.31	0.044	16q23	ADAM metallopeptidase with thrombospondin type 1 motif, 18
RGN	32.89	722.83	0.046	Xp11.3	Regulacin
FXYD2	38.92	845.24	0.046	11q23	FXYD domain containing ion transport regulator 2
LPL	217.26	4576.94	0.047	8p22	Lipoprotein lipase
TESC	945.69	19 893.72	0.048	12q24.22	Tescalcin

Table II. *Continued*

Gene abbreviation[b]	Median (poor prognosis)	Median (good prognosis)	Median fold change	Chromosomal location[c]	Gene name
SLC1A2	15.33	264.78	0.058	11p13–p12	Solute carrier family 1
ELMO1	65.12	1095.59	0.059	7p14.1	Engulfment and cell motility 1
MT1F	652.32	10 455.69	0.062	16q13	Metallothionein 1F
PGC	7.31	106.22	0.069	6p21.1	Progastricsin
RELN	3.54	47.69	0.074	7q22	Reelin
MT1M	27.31	291.10	0.094	16q13	Metallothionein 1M
MRAS	273.50	2805.97	0.097	3q22.3	Muscle RAS oncogene homolog
MCTP2	36.37	359.79	0.101	15q26.2	Multiple C2 domains, transmembrane 2
C10orf114	66.79	657.29	0.102	10p12.31	Overlapping with MiRNA1915
CA4	12.71	123.79	0.103	17q23	Carbonic anhydrase IV
GHSR	48.72	451.47	0.108	3q26.31	Growth hormone secretagogue receptor
EFCAB10	3.51	31.72	0.111	7q22.3	EFCAB10: EF-hand calcium-binding domain 10
DNAJC22	204.18	1739.58	0.117	12q13.12	DnaJ (Hsp40) homolog, subfamily C, member 22 (wurst)
PLAG1	125.83	1056.82	0.119	8q12	Pleiomorphic adenoma gene 1
SCTR	7.22	59.12	0.122	2q14.1	Secretin receptor
TSC22D1	51.99	400.74	0.130	13q14	TSC22 domain family, member 1
MPPED2	12.60	94.69	0.133	11p13	Metallophosphoesterase domain containing 2
LRRFIP1	62.69	459.87	0.136	2q37.3	Leucine rich repeat (in FLII) interacting protein 1
MT1G	1486.93	10 773.20	0.138	16q13	Metallothionein 1G
STOX1	51.59	368.36	0.140	10q22.1	Storkhead box 1, DNA-binding domain
VSTM2L	144.95	991.69	0.146	20q11.23	V-set and transmembrane domain containing 2 like
LRRFIP1	112.75	628.40	0.179	2q37.3	Leucine rich repeat (in FLII) interacting protein 1
SERPINE2	87.04	470.24	0.185	2q33–q35	Serpin peptidase inhibitor, clade E (nexin, plasminogen activator inhibitor type 1), member 2
FRMPD1	17.37	93.80	0.185	9p13.2	FERM and PDZ domain containing 1
MT1X	157.63	844.65	0.187	16q13	Metallothionein 1X
MAN2A1	93.32	468.95	0.199	5q21–q22	Mannosidase, alpha, class 2A, member 1

[a]The genes displayed here were selected from the 307 differentially expressed genes displayed in Supplementary Table S1, available at *Carcinogenesis* Online. Selected genes are annotated, display a median fold change difference in expression levels ≥5 and have an expression level ≥200 for at least one of the samples. When multiple probes and/or amplicons showed a significantly different expression, only the probe displaying the largest median fold change difference is listed.
[b]Gene abbreviations.
[c]Source of chromosomal locations shown in this table: UCSC genome browser (UCSC Genome Bioinformatics, version GRCh37/hg19, Santa Cruz, CA).

Of the 48 genes downregulated with a median fold change ≥5 in the poor prognosis group, 6 were located on chromosome 11q and 4 were members of the gene family of metallothioneins, i.e. *MT1F*, *MT1G*, *MT1M* and *MT1X* (Table II). Also the tumor suppressor genes *ADAMTS18*, *RELN* and *SOD3* were strongly downregulated in this group.

Validation of gene expression profiling results by qRT–PCR

To examine whether the results of the microarray study are reproducible, we performed qRT–PCR on the same 10 cases for a subset of up- and downregulated genes identified in the microarray. The downregulated genes *CD44* (10), *FOLR1*, *IL20RA*, *MT1F*, *OTP* (10) and *PCK1*, as well as the upregulated *BIRC5*, *BUB1*, *FANCA*, *KLK12* and *RET* (10) genes were selected from those listed in Table II based on their fold change in gene expression and/or their possible role(s) in disease progression. The microarray results could be reproduced for all genes tested, i.e. the expression trends were confirmed in the majority of the samples (Supplementary Table S3, available at *Carcinogenesis* Online). In addition, the prognostic value of the expression of the 11 selected genes was tested using qRT–PCR on an additional group of 55 carcinoid tumors. The qRT–PCR data were correlated with clinical patient follow-up data, when available. Using the Kaplan–Meier method, all genes described above were significantly associated with prognosis as shown in Figure 1 and as described previously for *CD44*, *OTP* and *RET* (10). In multivariate analyses, comparing the individual genes with clinical parameters (age at diagnosis, diameter, histopathology, sex), *BIRC5* ($P = 0.0066$), *BUB1* ($P = 0.0023$), *CD44* ($P = 0.012$), *IL20RA* ($P = 0.036$), *KLK12* ($P = 0.030$) and *OTP* ($P = 0.032$) were independent predictors of patient outcome. These findings were also validated at the protein level by immunohistochemical staining of CD44 and OTP, which were shown to be powerful prognostic indicators for lung carcinoids (10).

Thus, the microarray results were confirmed by qRT–PCR both through the prognostic value of a selection of 11 differentially expressed genes and by the similar ranking of their expression levels for the 10 samples (Supplementary Table S3, available at *Carcinogenesis* Online).

Identification of signaling pathways underlying carcinoid progression

Key pathways involved in carcinoid progression were queried by linking the list of 307 differentially expressed genes (Supplementary Table S1, available at *Carcinogenesis* Online) to the KEGG pathway database (http://www.genome.jp/kegg) using the online DAVID annotation tool (http://david.abcc.ncifcrf.gov/). Cell cycle and DNA damage detection and repair pathways were significantly altered (data not

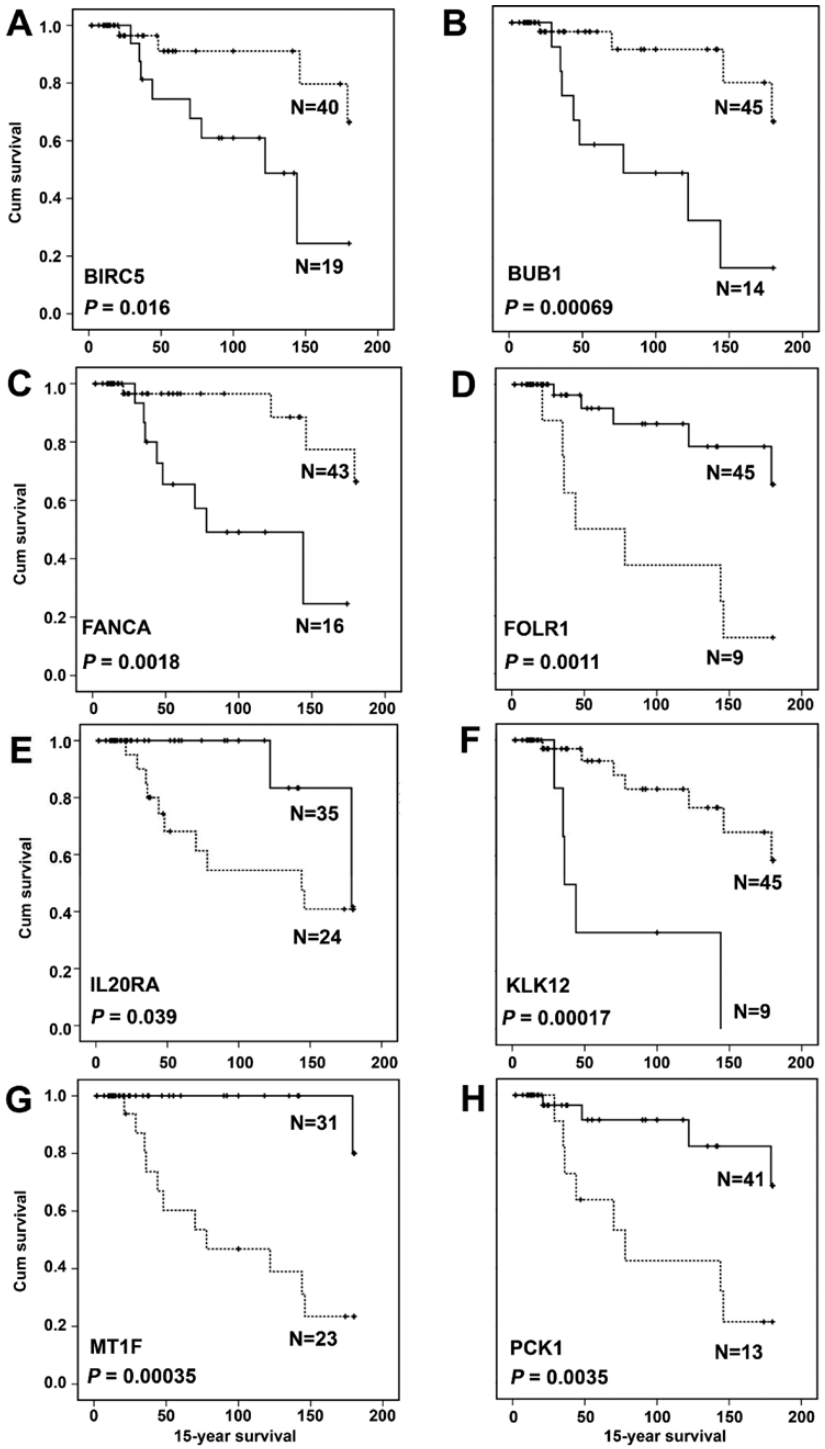

Fig. 1. Survival analyses of pulmonary carcinoids based on qRT–PCR of genes differentially expressed between tumors with a favorable and a poor prognosis. Kaplan–Meier survival analyses of pulmonary carcinoid tumors depicting the difference in 15 year overall survival for high (solid lines) or low (dotted lines) mRNA levels of a selection of differentially expressed genes relative to the geometric mean of *ACTB* and *CYPA*, and the sample with the highest expression (see Supplementary Materials and methods, available at *Carcinogenesis* Online). Optimal cutoff values were determined based on area under the receiver operating characteristic curve analyses. These cutoff points were 0.0020 for *BIRC5* (**A**), 0.0078 for *BUB1* (**B**), 0.012 for *FANCA* (**C**), 0.00080 for *FOLR1* (**D**), 0.15 for *IL20RA* (**E**), 0.0070 for *KLK12* (**F**), 0.018 for *MT1F* (**G**) and 0.0011 for *PCK1* (**H**).

shown). These pathways included well-known cancer-related genes, such as *CDK1/2*, cyclins and *TP53*, which were upregulated in carcinoids with a poor prognosis (Supplementary Table S1, available at *Carcinogenesis* Online). Strikingly, except for *BUB1*, none of the 71 top candidates shown in Table II were annotated to these pathways. Therefore, we performed an extensive manual literature search in combination with the online BioGRID tool (http://thebiogrid.org/) for protein interactions. As a result, a network of four interconnected pathways related to mitotic control mechanisms could be inferred from upregulated genes (Figure 2). This network included genes involved in (i) the mitotic spindle checkpoint (MSC); (ii) the CPC; (iii) mitotic kinase CDC2 activity and (iv) the BRCA-Fanconi

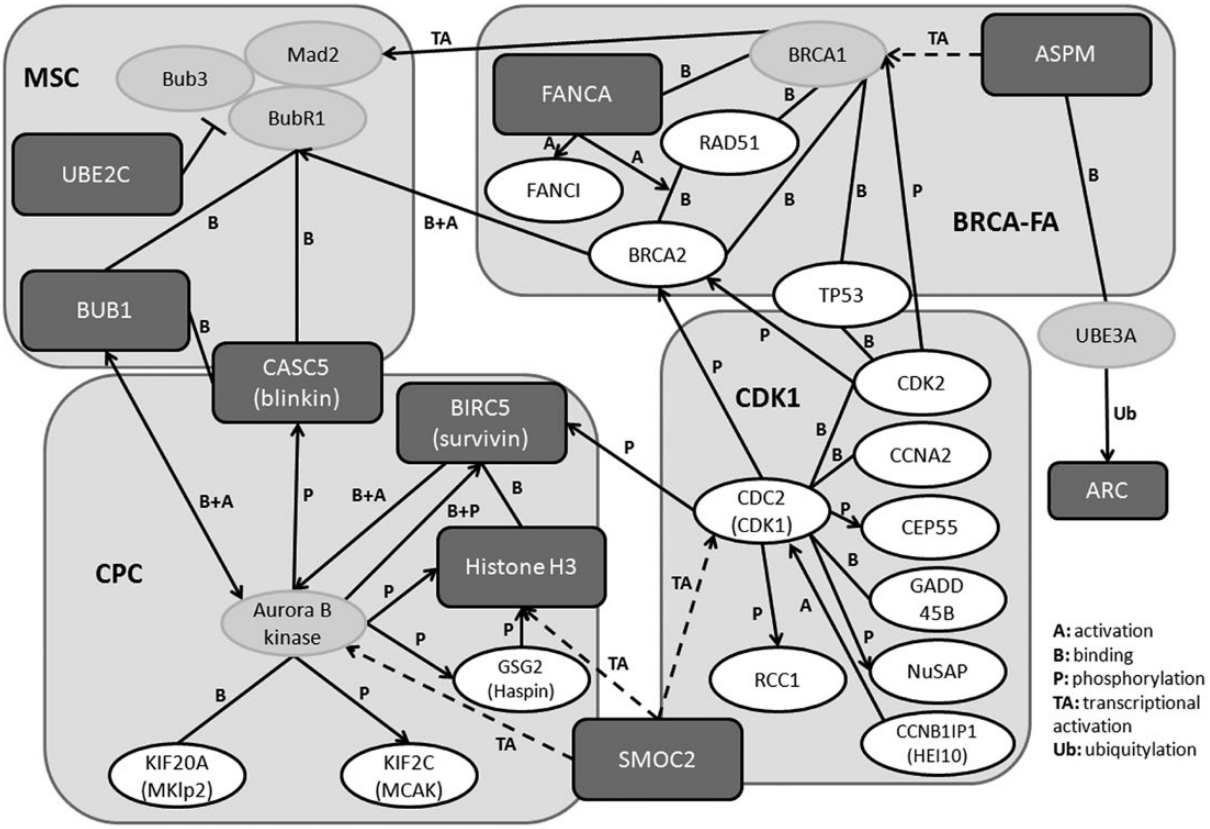

Fig. 2. Pathways related to lung carcinoid progression. Relationships between proteins encoded by upregulated genes in carcinoid tumors with an adverse disease outcome were compiled from data in the literature. Note that only relevant parts of the pathways are shown. The genes are taken from the lists in Table II (≥5-fold higher expressed in carcinoids with a poor prognosis; depicted as dark boxes) and Supplementary Table S1, available at *Carcinogenesis* Online (white circles). Genes in gray circles were not upregulated in our microarray but are related to multiple upregulated genes. B (for binding) indicates physical interactions between proteins. When these interactions lead to a phosphorylation event, this is indicated by P. TA indicates activation at the transcriptional (mRNA) level and A indicates posttranscriptional activation, whereas a bar-headed line indicates repression. UB indicates that the factor referred to is targeted to proteasomal degradation by the other factor, e.g. by ubiquitylation. The identified interactions between the depicted factors are summarized in the Supplementary Figure S2, available at *Carcinogenesis* Online.

anemia (FA) pathway. The identified interactions between the individually upregulated factors involved in these pathways are depicted in Figure 2 and justified in Supplementary Figure S2, available at *Carcinogenesis* Online.

Some of the genes from these pathways, i.e. *BIRC5*, *BUB1* and *FANCA*, were validated by qRT–PCR as described above and found to be upregulated in poor prognostic cases (see Figure 1).

Upregulation of mitotic genes in relation to chromosomal instability

Alterations of the MSC and CPC proteins have been reported to provoke chromosomal instability (CIN) (24,25). To identify chromosomal alterations in the 10 cases subjected to gene expression profiling, we performed high-resolution array CGH. The five carcinoid cases with a good prognosis generally exhibited low numbers of chromosomal alterations (≥10 Mb; mean 3, range 0–11; Supplementary Figure S1A, available at *Carcinogenesis* Online), whereas the five poor prognosis cases displayed a higher variability in the numbers of alterations (mean 12, range 0–27) (Table IC). Unexpectedly, one of the aggressive tumors (case 2) did not show major chromosomal alterations (Supplementary Figure S1B, available at *Carcinogenesis* Online), whereas two other poor prognosis cases (cases 1 and 4) displayed CIN, defined as described previously (9) (Supplementary Figure S1C, available at *Carcinogenesis* Online). These two cases exhibited higher expression of a number of mitotic genes than the other samples (without CIN), most notably *ASPM* and *UBE2C* (Supplementary Table S1, available at *Carcinogenesis* Online). Together, these data suggest a possible relationship between the upregulation of mitotic genes and CIN.

Amplifications (high copy number gains) and homozygous deletions of chromosomal regions were rare in the carcinoid cases. Five different amplifications and two homozygous deletions (present in at least two cases) could be identified (Table IC), including 8p11.2 that was homozygously deleted in four cases.

Upregulation of CPC components in relation to prognosis

As described above and shown in Figure 2, several of the upregulated genes, including *BIRC5* (survivin), could be linked to the CPC, with its major enzymatic component being ABk. This component was in itself not differentially expressed by the five cases with a poor outcome.

To further examine the role of the CPC in carcinoid progression, the messenger RNA (mRNA) expression levels of *AURKB* and *BIRC5* were analyzed in 65 carcinoid tumors and found to be strongly correlated with each other ($P < 1e^{-36}$, Pearson's correlation; Figure 3A and B) and with prognosis (see Figure 1A for *BIRC5* and Figure 3C for *AURKB*). In general, low expression levels were evident for both genes in carcinoids, whereas considerably higher expression levels were only present in a few ACs (Figure 3A and B), as well as in the carcinoid cell lines H720 and H727 (Figure 3D and E).

Protein expression levels of ABk and survivin were assessed in 50 carcinoids by immunohistochemical staining (Figure 4A–C and Supplementary Table S4, available at *Carcinogenesis* Online) and again, a strong correlation between the expression of both proteins was seen ($P = 7.2e^{-15}$, Pearson's correlation). ABk as well as survivin could exhibit nuclear and/or cytoplasmic reactivity. Nuclear ABk expression was present in ≤5% of nuclei of

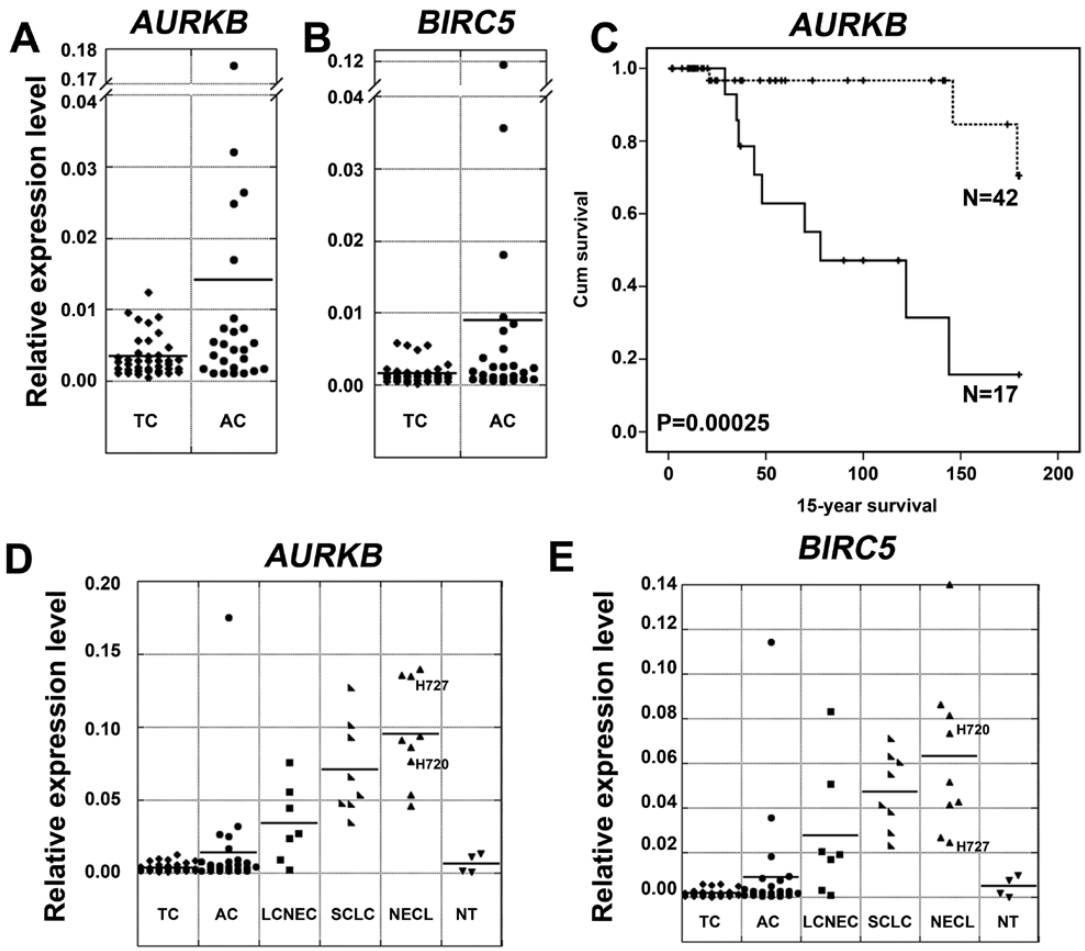

Fig. 3. Gene expression levels of *AURKB* and *BIRC5* in pulmonary NENs. (**A** and **B**) qRT–PCR results for *AURKB* and *BIRC5* in typical carcinoids (TC) and ACs. (**C**) Kaplan–Meier survival analysis plot depicting the differences in 15 year overall survival for high (solid line) or low (dotted line) *AURKB* gene expression levels within the group of pulmonary carcinoid tumors. Cutoff level based on area under the receiver operating characteristic curve: 0.0051. (**D** and **E**) qRT–PCR results for TCs, ACs, large cell neuroendocrine carcinomas, SCLC, neuroendocrine cell lines (NECL) and normal tissue (NT) for *AURKB* and *BIRC5*. mRNA expression levels are relative to the geometric mean of *ACTB* and *CYPA* and the sample with the highest expression (see Supplementary Materials and methods, available at *Carcinogenesis* Online). The mean values are indicated by the horizontal bars.

most carcinoid tumors (Figure 4A), with the exception of three cases (Figure 4B). Two of these three cases were included in the qRT–PCR and array CGH series and also exhibited higher mRNA levels, as well as CIN. The case with the highest mRNA expression, however, displayed strong cytoplasmic reactivity only (Figure 4C). Although the disease outcome for cases displaying ABk-positive cell frequencies >1% tended to be slightly worse (Figure 4D), the difference with cases without nuclear ABk reactivity was not significant.

The number of positive nuclei for survivin was on average higher as compared with ABk (3.6 and 1.7%, respectively), as could be expected from the microarray data. Only few cases showed expression in >10% of nuclei (Supplementary Table S4, available at *Carcinogenesis* Online and Figure 4B). A number of cases exhibited a prominent cytoplasmic staining reactivity for survivin (Supplementary Table S4, available at *Carcinogenesis* Online). Again, the case with the highest gene expression levels displayed strong cytoplasmic reactivity, but almost no nuclear expression (Figure 4D). Survivin protein expression in cases with >2.5% positive nuclei was also related to poor disease outcome (Figure 4D).

At the mRNA level, both *AURKB* (P = 0.00063, 95% confidence interval = 0.0279–0.0843) and *BIRC5* (P = 0.000049, 95% confidence interval = 0.0220–0.0505) were significantly higher expressed in neuroendocrine lung carcinomas as compared with the carcinoids (Figure 3D and E). Fifteen high-grade neuroendocrine carcinomas were analyzed for ABk and survivin protein expression using immunohistochemistry (Supplementary Table S4, available at *Carcinogenesis* Online). Although not all carcinomas showed staining for ABk, these tumors exhibited positivity in a much higher number of cases, and for the individual cases in a much higher frequency of nuclei (mean 25%, range 0–59%; Figure 4E). The same holds true for survivin (mean 40%, range 22–74%; Figure 4E).

Downregulation of 11q-located genes

Three out of five samples with a poor prognosis displayed deletion of chromosome 11q, reported previously as an indicator of adverse disease outcome in carcinoids (9). Significantly more downregulated genes are located on this chromosome arm as compared with other chromosome arms (P = 0.00017; Supplementary Table S5, available at *Carcinogenesis* Online). With the exception of *FOLR1*, the genes that were downregulated >5 times (Table II) displayed a tendency toward lower expression in the three cases combining a poor prognosis with a deletion of 11q, as compared with the two poor prognosis cases not containing this deletion (Supplementary Table S1, available at *Carcinogenesis* Online). This could indicate that the loss of one 11q chromosome arm is (partly) responsible for the further decrease in gene expression, although this needs to be confirmed on larger tumor series.

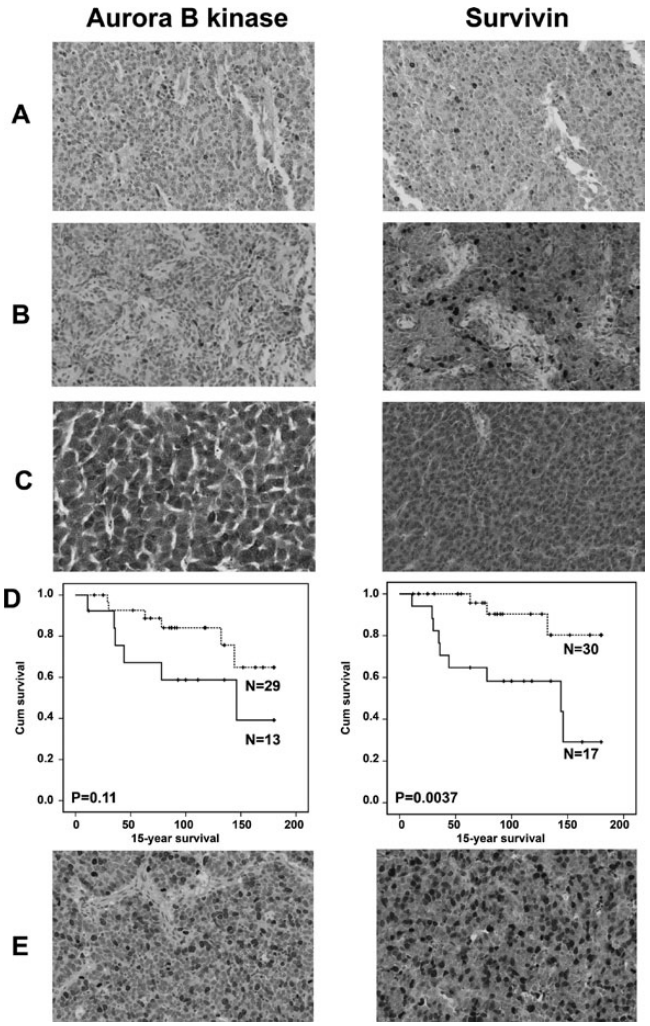

Fig. 4. ABk and survivin protein expression in pulmonary NENs and their relation to patient outcome. (**A**–**C**) Immunohistochemistry results of carcinoid tumors. (**A**) AC with a favorable prognosis (case 8), exhibiting nuclear reactivity in a small number of cells for both proteins. In addition, this case exhibits cytoplasmic reactivity for survivin. (**B**) Metastatic AC showing nuclear reactivity in a considerable fraction of cells for both proteins, with a higher frequency for survivin than for ABk. (**C**) AC with the highest gene expression for both *AURKB* and *BIRC5* (see Figure 3A and B). This case has almost no positive nuclei but exhibits a strong cytoplasmic expression for both proteins. (**D**) Kaplan–Meier survival analyses of pulmonary carcinoid tumors depicting the difference in 15 year overall survival for high (solid lines) or low (dotted lines) protein expression levels of ABk and survivin. The cutoff value for ABk was arbitrarily set at 1% positive nuclei, whereas the cutoff value for survivin protein expression was determined at 2.5% based on area under the receiver operating characteristic curve analyses. (**E**) Immunohistochemistry result in a high-grade neuroendocrine carcinoma showing strong nuclear reactivity for both proteins. All original magnifications were ×200.

Discussion

This is the first gene expression profiling report focusing on the progression of pulmonary carcinoid tumors. The prognostic value of a number of candidate genes could be validated, whereas specific signaling routes could be associated with the more aggressive behavior of carcinoids. In cases with adverse disease outcome, upregulated genes could be assigned to mitotic control pathways. In addition, multiple tumor suppressor genes and genes located at 11q were downregulated.

Downregulated genes located at 11q

As compared with other genomic regions, significantly more downregulated genes were located at chromosome 11q. In addition to *MEN1* mutations involved in the carcinogenesis of a subset of sporadic lung carcinoids (1,26), the presence of an additional tumor suppressor gene at 11q13 has since long been hypothesized because frequencies of loss of heterozygosity at 11q13 are higher than *MEN1* mutation frequencies (26). Using qRT–PCR we observed earlier that *MEN1* is indeed downregulated in carcinoids with a poor prognosis (27). Of the genes located at this chromosomal region, *FOLR1* and *FOLR3* were >5 times downregulated in the aggressive carcinoids. *FOLR1* encodes the folate receptor α and is expressed in various epithelial tumors, whereas both *FOLR1* and *FOLR3* are highly expressed in ovarian carcinomas (28). Also in lung adenocarcinomas, higher expression of *FOLR1* is associated with a favorable disease outcome (29).

Based on our previous study (9), candidate tumor suppressor genes at the telomeric part of chromosome 11q were also expected. A number of genes at this locus were >5 times downregulated, including discs large homolog 2 (*DLG2*) at 11q14.1. This gene encodes a membrane-associated guanylate kinase involved in establishing and maintaining cell polarity in epithelial cells and neurons. Both FXYD domain containing ion transport regulator 2 (*FXYD2*), the gamma-subunit of the NaK-ATPase, at 11q23, and Kin of IRRE like 3 (*KIRREL3*, also known as NEPH2) at 11q24 are expressed in dorsal root ganglions (30,31). The latter is a transmembrane protein involved in neuronal migration in the pontine nucleus and may play a role in axonal path finding and synapse formation of dorsal root ganglion neurons on appropriate targets (31,32). Beta-1,3-glucuronyltransferase 1 (*B3GAT1*, also known as *CD57* and *Leu7*) is located at 11q25. Although CD57 positivity is mainly present on natural killer cells, Bunn *et al.* (33) demonstrated in an early study that the majority of SCLCs, as well as six out of six carcinoids (without clinical information) tested were positive for this factor.

In addition to 11q deletion, some novel amplifications and homozygous deletions could be identified in this study. For example, *ADAM3A* and *ADAM5P* (8p11.22) were homozygously deleted in four cases. This region was not identified in our previous report (9) due to higher resolution of the array CGH in the underlying study. *ADAM3A* was previously reported to be prone to homozygous loss in gliomas (34). Case 1 had an amplification of *MYC* at 8q24.21, as shown previously (9).

Pathways related to progression of pulmonary carcinoids

A network comprising of mitotic genes and BRCA-related genes was found to be upregulated in carcinoid tumors with a poor disease outcome (Figure 2). We studied a number of factors involved in this network in more detail by qRT–PCR and immunohistochemistry. The four identified pathways, i.e. the CPC, the MSC, CDK2 and BRCA-FA pathway, have been thoroughly reviewed elsewhere (24,25,35–39), and the relationships between the factors upregulated in the microarray experiments and involved in these signaling routes have been described in Supplementary Figure S2, available at *Carcinogenesis* Online.

In short, the CPC consists of ABk and three non-enzymatic subunits, i.e. borealin, survivin and INCENP (36). These latter three factors control the activity, stability and targeting of ABk. The CPC has many functions during mitosis. Although initially located at chromosome arms, the complex is transferred during (pro)metaphase to the inner centromeres. Its most important function is probably the regulation of kinetochore–microtubule attachments, where it can sense a lack of tension caused by inappropriate microtubule attachments, leading to mitotic arrest. However, the CPC is also indispensable for other stages of the cell cycle, e.g. mitotic spindle formation and completion of cytokinesis (36).

The MSC functions to enable proper chromosome separation during mitosis by controlling the attachment of the kinetochores of the individual chromosomes to the mitotic spindle (24,35). The core mitotic checkpoint complex consists of BUB3, BUBR1, CDC20 and MAD2 and inhibits the anaphase-promoting complex/cyclosome, preventing the start of the anaphase until all chromosomes are properly segregated (35). Although none of the core members of the mitotic checkpoint complex were upregulated in this microarray experiment, several associated factors, such as *CASC5* and *BUB1*, did show increased mRNA levels.

In the BRCA-FA pathway, BRCA1, BRCA2 and RAD51 cooperate with the FA proteins in response to DNA damage to preserve chromosomal stability (38). FANCA is a member of the core complex of FA proteins. This complex monoubiquitylates FANCD2 and FANCI, which migrate subsequently to foci also containing BRCA1, BRCA2 and RAD51 in the nuclei of cells that have accumulated DNA damage (37,38).

Finally, several factors related to the main mitotic kinase CDC2/CDK1 were upregulated, albeit <5 times. CDK1 is the main mitotic kinase and is activated by A-type cyclins at the end of interphase (39). It functions as a master regulator of mitosis and among its phosphorylation targets are >70 different substrates. After the MSC has ensured that all chromosomes are correctly attached to the mitotic spindle, CDK1 is inactivated through degradation of cyclin B.

It can be envisaged that slight alterations in the four interconnected pathways may have large effects on cell division and may therefore be involved in the progression of carcinoids. Several genes upregulated ≥5 times in the identified network (Figure 2) have been described in the context of cancer. The *CASC5* gene is upregulated in several types of cancer, including lung cancer, where it is associated with poor differentiation and smoking (40). BUB1 overexpression, found to be related to an adverse disease outcome, promotes hyperactivity of ABk and induces tumor formation in transgenic mice (41), whereas *BUB1* mutations have been identified in colorectal cancer cell lines (42). Overexpression of UBE2C, shown in several types of cancer, is known to cause chromosome lagging, aneuploidy and tumor formation in mice (43). Increased mRNA levels of *ASPM* have been reported in glioblastomas, and its inhibition was shown to repress tumor cell proliferation (44). SMOC-2 may be an angiogenic factor and was shown to upregulate among others histone H3, *AURKB* and *CDC2* transcription when transduced into human umbilical vein endothelial cells (45).

In pulmonary carcinoids, increased mRNA levels of *AURKB* and *BIRC5* were related to low survival rates. With respect to protein levels, a significant relation with patient outcome was found for nuclear expression of survivin. For ABk, nuclear staining in carcinoid tumors was generally low, whereas most neuroendocrine carcinomas displayed stronger immunoreactivity. Survivin is overexpressed in many cancer types, including lung tumors (46). Although the expression of survivin has been extensively studied in non-SCLC (NSCLC) (47), reports on its expression in neuroendocrine lung tumors are consistently lacking and also, to our knowledge, data on the expression of survivin in pulmonary carcinoids and large cell neuroendocrine carcinoma have not been previously published. Halasova *et al.* (48) recently reported lower frequencies and staining intensities in SCLCs as compared with other types of lung cancer, whereas Belyanskaya *et al.* (49) reported higher gene expression levels in SCLC cell lines as compared with NSCLC cell lines. Overexpression of ABk has been reported in NSCLC (50,51), but data on its expression have not been reported in (primary) lung NENs.

Next to genes located at chromosome 11q or involved in the four pathways, also a few other genes were validated as possible prognostic indicators for pulmonary carcinoids. Of these, *CD44*, *OTP* and *RET* were discussed previously (10). Although *RET* was the strongest upregulated gene in the underlying study, it could not be directly related to other differentially expressed genes, although some of them may be among its downstream targets. KLK12 is a secreted serine protease (52), found to be upregulated in prostate cancer (53) and recently reported as a prognostic indicator for gastric cancer (54). Among its targets are matricellular proteins of the CCN (CYR61-CTGF-NOV) family (52). IL20-RA is one of the two subunits comprising together the IL20-receptor (55). These receptor subunits are upregulated in psoriatic skin, but individual functions for IL20-RA have not been described. *MT1F* is a member of the gene family of metallothioneins, from which also *MT1G*, *MT1M* and *MT1X* were significantly lower expressed in the messenger RNA microarray. Both tumor suppressive and oncogenic functions have been assigned to members of the MT1 family of proteins (56), including MT1F (57,58). *PCK1* has been described to be downregulated in colon cancer (59).

Relation of mitotic pathway alterations to CIN and Ki-67 proliferation index

Alterations of both the MSC and CPC proteins have been reported to cause CIN (24,25) and both up- and downregulation of CPC members, including ABk, may cause this effect (60). Two of the five poor prognosis samples displayed extensive CIN and in these cases a stronger upregulation of a number of genes involved in the described pathways, particularly *ASPM* and *UBE2C*, was evident. These cases had in addition considerable mRNA expression levels of the MSC component *BUB1* and the CPC components *AURKB* and *BIRC5*, which is in agreement with studies in NSCLC, where higher gene expression of *AURKB* has been demonstrated in tumors with genomic instability (50). Also SCLCs and large cell neuroendocrine carcinomas, tumors known to frequently exhibit CIN (1), demonstrated high gene expression levels of *AURKB* and *BIRC5*. In gene expression profiling studies conducted on SCLCs, the MSC components *BUB1B* and *MAD2L1* were reported to be upregulated (61,62).

The same carcinoid cases that displayed CIN had an increased Ki-67 index. These cases were consensus classified as ACs by two experienced pathologists and were diploid in nature (9). However, they may represent borderline cases between ACs and high-grade lung NENs. This view is supported by the fact that one of these cases showed *MYC* amplification (9) and *TP53* mutation, which are usually hallmarks of high-grade lung NENs (1,9). Carcinoid tumors exhibit usually <20% Ki-67-positive cells, but for ACs higher frequencies have also been reported (12). Ki-67 is currently not a discriminative criterion between carcinoids and high-grade pulmonary neuroendocrine carcinomas (2). Furthermore, CIN is not necessarily associated with a poor prognosis, as we have demonstrated previously (9).

Conclusion and future prospects

This study provides the first unmasking of possible genes involved in the malignant progression of lung carcinoids. We report several genes that may serve as novel prognostic markers, including downregulated candidates on chromosome 11q, a locus earlier described to be frequently lost in aggressive cases (9). *BIRC5*, *BUB1*, *CD44*, *IL20RA*, *KLK12* and *OTP* are found to be independent predictors of patient outcome. Moreover, pathway analysis showed the involvement of signaling routes related to mitotic control mechanisms in carcinoid progression, different from those mostly observed in carcinomas (63). These include the CPC and the MSC. Their upregulation is suggested to be related to CIN and enhanced proliferation.

Taking together this data, it is tempting to speculate about the driving factor(s) of carcinoid progression. Strong candidates include the tyrosine kinase receptor *RET*, which stimulates many downstream pathways and is most strongly upregulated in the microarray experiment (10), as well as *SMOC2*, which upregulates *AURKB*. Further studies should focus on the identification of genes driving oncogenesis of pulmonary carcinoids and separate these from the passenger genes that have merely secondary effects on tumorigenesis.

Increased levels of ABk and survivin, both central in the CPC, were associated with poor disease outcome in the group of carcinoids. There are several lines of evidence that ABk and survivin may be therapeutic targets, also for neuroendocrine lung tumors. SCLC cell lines, particularly those with upregulation of one of the three *MYC* genes, are sensitive to the Aurora kinase inhibitor PF-03814735 (64). Recently, Sos *et al.* (65) have demonstrated that *MYC*-amplified SCLC cell lines are also sensitive to other Aurora kinase inhibitors and that the activity of these inhibitors is mainly dependent on ABk. Interestingly, one of the carcinoids with high ABk expression displays *MYC* amplification (9). Because survivin is not expressed by most normal adult tissues, it is also an attractive target for therapeutic intervention (46). Survivin inhibitors are currently under evaluation in clinical trials for several types of cancer (66), in which lung NENs, more in particular the high-grade carcinomas, could be included.

Supplementary material

Supplementary Materials and methods, Tables S1–S5 and Figures S1 and S2 can be found at http://carcin.oxfordjournals.org/

Funding

Jan Dekkerstichting & Ludgardine Bouwmanstichting (nr. 2010_010).

Acknowledgements

We thank Francois Rustenburg and Rinus Voorham, Department of Pathology, VU University Medical Center, Amsterdam, The Netherlands, for help with the gene expression arrays and the array CGH. Guido Roemen and Tina Pirens, Department of Pathology, Maastricht University Medical Center, Maastricht, The Netherlands, are acknowledged for performing *TP53* mutation analysis. Kim Smits, Department of Radiation Oncology (MAASTRO Clinic), Maastricht University Medical Center, Maastricht, The Netherlands, is acknowledged for assistance with statistical analyses. We furthermore thank Anne-Marie Dingemans, Department of Pulmonology, Maastricht University Medical Center, Maastricht, The Netherlands, for clinical patient follow-up data, and Robert-Jan van Suylen, Department of Pathology, Jeroen Bosch Hospital, 's-Hertogenbosch, and Erik Thunnissen, Department of Pathology, VU Medical Center, Amsterdam, The Netherlands, for tumor reclassifications.

Conflict of Interest Statement: W.V.C. is employed as CSO in MdxHealth. E.-J.M.S. has honoraria from Speakers Bureau of Pfizer and Lilly and is a consultant/advisory board member of Pfizer.

References

1. Swarts,D.R. *et al.* (2012) Molecular and cellular biology of neuroendocrine lung tumors: evidence for separate biological entities. *Biochim. Biophys. Acta*, **1826**, 255–271.
2. Beasley,M.B. *et al.* (2004) Carcinoid tumour. In Travis,W.D. *et al.* (eds) *Pathology and Genetics of Tumours of the Lung, Pleura, Thymus and Heart*. IARC Press, Lyon, pp. 59–62.
3. Travis,W.D. (2010) Advances in neuroendocrine lung tumors. *Ann. Oncol*., **21** (suppl. 7), vii65–vii71.
4. Detterbeck,F.C. (2010) Management of carcinoid tumors. *Ann. Thorac. Surg*., **89**, 998–1005.
5. Debelenko,L.V. *et al.* (1997) Identification of MEN1 gene mutations in sporadic carcinoid tumors of the lung. *Hum. Mol. Genet*., **6**, 2285–2290.
6. Srirajaskanthan,R. *et al.* (2009) Surgical management and palliative treatment in bronchial neuroendocrine tumours: a clinical study of 45 patients. *Lung Cancer*, **65**, 68–73.
7. Lim,E. *et al.* (2008) Proceedings of the IASLC International Workshop on Advances in Pulmonary Neuroendocrine Tumors 2007. *J. Thorac. Oncol*., **3**, 1194–1201.
8. Beasley,M.B. *et al.* (2000) Pulmonary atypical carcinoid: predictors of survival in 106 cases. *Hum. Pathol*., **31**, 1255–1265.
9. Swarts,D.R. *et al.* (2011) Deletions of 11q22.3-q25 are associated with atypical lung carcinoids and poor clinical outcome. *Am. J. Pathol*., **179**, 1129–1137.
10. Swarts,D.R. *et al.* (2013) CD44 and OTP are strong prognostic markers for pulmonary carcinoids. *Clin. Cancer Res*., **19**, 2197–2207.
11. Brambilla,E. *et al.* (1996) Apoptosis-related factors p53, Bcl2, and Bax in neuroendocrine lung tumors. *Am. J. Pathol*., **149**, 1941–1952.
12. Walts,A.E. *et al.* (2012) Limited role of Ki-67 proliferative index in predicting overall short-term survival in patients with typical and atypical pulmonary carcinoid tumors. *Mod. Pathol*., **25**, 1258–1264.
13. Zahel,T. *et al.* (2012) Phenotyping of pulmonary carcinoids and a Ki-67-based grading approach. *Virchows Arch*., **460**, 299–308.
14. Granberg,D. *et al.* (2000) Prognostic markers in patients with typical bronchial carcinoid tumors. *J. Clin. Endocrinol. Metab*., **85**, 3425–3430.
15. Van 't Veer,L.J. *et al.* (2002) Gene expression profiling predicts clinical outcome of breast cancer. *Nature*, **415**, 530–536.
16. Anbazhagan,R. *et al.* (1999) Classification of small cell lung cancer and pulmonary carcinoid by gene expression profiles. *Cancer Res*., **59**, 5119–5122.
17. Bhattacharjee,A. *et al.* (2001) Classification of human lung carcinomas by mRNA expression profiling reveals distinct adenocarcinoma subclasses. *Proc. Natl Acad. Sci. USA*, **98**, 13790–13795.
18. Jones,M.H. *et al.* (2004) Two prognostically significant subtypes of high-grade lung neuroendocrine tumours independent of small-cell and large-cell neuroendocrine carcinomas identified by gene expression profiles. *Lancet*, **363**, 775–781.
19. He,P. *et al.* (2004) Identification of carboxypeptidase E and gamma-glutamyl hydrolase as biomarkers for pulmonary neuroendocrine tumors by cDNA microarray. *Hum. Pathol*., **35**, 1196–1209.
20. Virtanen,C. *et al.* (2002) Integrated classification of lung tumors and cell lines by expression profiling. *Proc. Natl Acad. Sci. USA*, **99**, 12357–12362.
21. Van Neste,L. *et al.* (2012) The epigenetic promise for prostate cancer diagnosis. *Prostate*, **72**, 1248–1261.
22. den Bakker,M.A. *et al.* (2013) Neuroendocrine tumours--challenges in the diagnosis and classification of pulmonary neuroendocrine tumours. *J. Clin. Pathol*, in press.
23. Travis,W.D. *et al.* (1991) Neuroendocrine tumors of the lung with proposed criteria for large-cell neuroendocrine carcinoma. An ultrastructural, immunohistochemical, and flow cytometric study of 35 cases. *Am. J. Surg. Pathol*., **15**, 529–553.
24. Kops,G.J. *et al.* (2005) On the road to cancer: aneuploidy and the mitotic checkpoint. *Nat. Rev. Cancer*, **5**, 773–785.
25. Lens,S.M. *et al.* (2010) Shared and separate functions of polo-like kinases and aurora kinases in cancer. *Nat. Rev. Cancer*, **10**, 825–841.
26. Görtz,B. *et al.* (1999) Mutations and allelic deletions of the MEN1 gene are associated with a subset of sporadic endocrine pancreatic and neuroendocrine tumors and not restricted to foregut neoplasms. *Am. J. Pathol*., **154**, 429–436.
27. Swarts,D.R. *et al.* (2011) Reduced MEN1 gene expression in pulmonary carcinoids is associated with metastatic disease. *Neuroendocrinology*, **94**, 12.
28. Yuan,Y. *et al.* (2009) Expression of the folate receptor genes FOLR1 and FOLR3 differentiates ovarian carcinoma from breast carcinoma and malignant mesothelioma in serous effusions. *Hum. Pathol*., **40**, 1453–1460.
29. Iwakiri,S. *et al.* (2008) Expression status of folate receptor alpha is significantly correlated with prognosis in non-small-cell lung cancers. *Ann. Surg. Oncol*., **15**, 889–899.
30. Ventéo,S. *et al.* (2012) Regulation of the Na,K-ATPase gamma-subunit FXYD2 by Runx1 and Ret signaling in normal and injured non-peptidergic nociceptive sensory neurons. *PLoS One*, **7**, e29852.
31. Komori,T. *et al.* (2008) Expression of kin of irregular chiasm-like 3/mKirre in proprioceptive neurons of the dorsal root ganglia and its interaction with nephrin in muscle spindles. *J. Comp. Neurol*., **511**, 92–108.
32. Nishida,K. *et al.* (2011) Role of Neph2 in pontine nuclei formation in the developing hindbrain. *Mol. Cell. Neurosci*., **46**, 662–670.
33. Bunn,P.A. Jr *et al.* (1985) Small cell lung cancer, endocrine cells of the fetal bronchus, and other neuroendocrine cells express the Leu-7 antigenic determinant present on natural killer cells. *Blood*, **65**, 764–768.
34. Barrow,J. *et al.* (2011) Homozygous loss of ADAM3A revealed by genome-wide analysis of pediatric high-grade glioma and diffuse intrinsic pontine gliomas. *Neuro. Oncol*., **13**, 212–222.
35. Musacchio,A. *et al.* (2007) The spindle-assembly checkpoint in space and time. *Nat. Rev. Mol. Cell Biol*., **8**, 379–393.
36. Ruchaud,S. *et al.* (2007) Chromosomal passengers: conducting cell division. *Nat. Rev. Mol. Cell Biol*., **8**, 798–812.
37. Garner,E. *et al.* (2011) Ubiquitylation and the Fanconi anemia pathway. *FEBS Lett*., **585**, 2853–2860.
38. Venkitaraman,A.R. (2004) Tracing the network connecting BRCA and Fanconi anaemia proteins. *Nat. Rev. Cancer*, **4**, 266–276.
39. Malumbres,M. *et al.* (2009) Cell cycle, CDKs and cancer: a changing paradigm. *Nat. Rev. Cancer*, **9**, 153–166.
40. Takimoto,M. *et al.* (2002) Frequent expression of new cancer/testis gene D40/AF15q14 in lung cancers of smokers. *Br. J. Cancer*, **86**, 1757–1762.
41. Ricke,R.M. *et al.* (2011) Bub1 overexpression induces aneuploidy and tumor formation through Aurora B kinase hyperactivation. *J. Cell Biol*., **193**, 1049–1064.
42. Cahill,D.P. *et al.* (1998) Mutations of mitotic checkpoint genes in human cancers. *Nature*, **392**, 300–303.
43. van Ree,J.H. *et al.* (2010) Overexpression of the E2 ubiquitin-conjugating enzyme UbcH10 causes chromosome missegregation and tumor formation. *J. Cell Biol*., **188**, 83–100.
44. Horvath,S. *et al.* (2006) Analysis of oncogenic signaling networks in glioblastoma identifies ASPM as a molecular target. *Proc. Natl Acad. Sci. USA*, **103**, 17402–17407.
45. Rocnik,E.F. *et al.* (2006) The novel SPARC family member SMOC-2 potentiates angiogenic growth factor activity. *J. Biol. Chem*., **281**, 22855–22864.
46. Altieri,D.C. (2003) Validating survivin as a cancer therapeutic target. *Nat. Rev. Cancer*, **3**, 46–54.

47. Huang,L.N. *et al.* (2013) Expression of survivin and patients survival in non-small cell lung cancer: a meta-analysis of the published studies. *Mol. Biol. Rep*., **40**, 917–924.
48. Halasova,E. *et al.* (2013) Expression of Ki-67, Bcl-2, survivin and p53 proteins in patients with pulmonary carcinoma. *Adv. Exp. Med. Biol*., **756**, 15–21.
49. Belyanskaya,L.L. *et al.* (2005) Cisplatin activates Akt in small cell lung cancer cells and attenuates apoptosis by survivin upregulation. *Int. J. Cancer*, **117**, 755–763.
50. Smith,S.L. *et al.* (2005) Overexpression of aurora B kinase (AURKB) in primary non-small cell lung carcinoma is frequent, generally driven from one allele, and correlates with the level of genetic instability. *Br. J. Cancer*, **93**, 719–729.
51. Vischioni,B. *et al.* (2006) Frequent overexpression of aurora B kinase, a novel drug target, in non-small cell lung carcinoma patients. *Mol. Cancer Ther*., **5**, 2905–2913.
52. Guillon-Munos,A. *et al.* (2011) Kallikrein-related peptidase 12 hydrolyzes matricellular proteins of the CCN family and modifies interactions of CCN1 and CCN5 with growth factors. *J. Biol. Chem*., **286**, 25505–25518.
53. Lose,F. *et al.* (2013) Common variation in Kallikrein genes KLK5, KLK6, KLK12, and KLK13 and risk of prostate cancer and tumor aggressiveness. *Urol. Oncol.*, **31**, 635–643.
54. Zhao,E.H. *et al.* (2012) Clinical significance of human kallikrein 12 gene expression in gastric cancer. *World J. Gastroenterol*., **18**, 6597–6604.
55. Blumberg,H. *et al.* (2001) Interleukin 20: discovery, receptor identification, and role in epidermal function. *Cell*, **104**, 9–19.
56. Pedersen,M.O. *et al.* (2009) The role of metallothionein in oncogenesis and cancer prognosis. *Prog. Histochem. Cytochem*., **44**, 29–64.
57. Werynska,B. *et al.* (2013) Metallothionein 1F and 2A overexpression predicts poor outcome of non-small cell lung cancer patients. *Exp. Mol. Pathol*., **94**, 301–308.
58. Yan,D.W. *et al.* (2012) Downregulation of metallothionein 1F, a putative oncosuppressor, by loss of heterozygosity in colon cancer tissue. *Biochim. Biophys. Acta*, **1822**, 918–926.
59. Blouin,J.M. *et al.* (2010) Down-regulation of the phosphoenolpyruvate carboxykinase gene in human colon tumors and induction by omega-3 fatty acids. *Biochimie*, **92**, 1772–1777.
60. Gautschi,O. *et al.* (2008) Aurora kinases as anticancer drug targets. *Clin. Cancer Res*., **14**, 1639–1648.
61. Rohrbeck,A. *et al.* (2008) Gene expression profiling for molecular distinction and characterization of laser captured primary lung cancers. *J. Transl. Med*., **6**, 69.
62. Taniwaki,M. *et al.* (2006) Gene expression profiles of small-cell lung cancers: molecular signatures of lung cancer. *Int. J. Oncol*., **29**, 567–575.
63. Peifer,M. *et al.* (2012) Integrative genome analyses identify key somatic driver mutations of small-cell lung cancer. *Nat. Genet*., **44**, 1104–1110.
64. Hook,K.E. *et al.* (2012) An integrated genomic approach to identify predictive biomarkers of response to the aurora kinase inhibitor PF-03814735. *Mol. Cancer Ther*., **11**, 710–719.
65. Sos,M.L. *et al.* (2012) A framework for identification of actionable cancer genome dependencies in small cell lung cancer. *Proc. Natl Acad. Sci. USA*, **109**, 17034–17039.
66. Mita,A.C. *et al.* (2008) Survivin: key regulator of mitosis and apoptosis and novel target for cancer therapeutics. *Clin. Cancer Res*., **14**, 5000–5005.

Received April 3, 2013; revised July 13, 2013; accepted August 1, 2013